



# Effects of Gastric Bypass Surgery on the Brain: Simultaneous Assessment of Glucose Uptake, Blood Flow, Neural Activity, and Cognitive Function During Normo- and Hypoglycemia

Kristina E. Almby,<sup>1</sup> Martin H. Lundqvist,<sup>1</sup> Niclas Abrahamsson,<sup>1</sup> Sofia Kvernby,<sup>2</sup> Markus Fahlström,<sup>2</sup> Maria J. Pereira,<sup>1</sup> Malin Gingnell,<sup>3</sup> F. Anders Karlsson,<sup>1</sup> Giovanni Fanni,<sup>1</sup> Magnus Sundbom,<sup>2</sup> Urban Wiklund,<sup>4</sup> Sven Haller,<sup>2,5</sup> Mark Lubberink,<sup>2</sup> Johan Wikström,<sup>2</sup> and Jan W. Eriksson<sup>1</sup>

*Diabetes* 2021;70:1265–1277 | <https://doi.org/10.2337/db20-1172>

**While Roux-en-Y gastric bypass (RYGB) surgery in obese individuals typically improves glycemic control and prevents diabetes, it also frequently causes asymptomatic hypoglycemia. Previous work showed attenuated counterregulatory responses following RYGB. The underlying mechanisms as well as the clinical consequences are unclear. In this study, 11 subjects without diabetes with severe obesity were investigated pre- and post-RYGB during hyperinsulinemic normo-hypoglycemic clamps. Assessments were made of hormones, cognitive function, cerebral blood flow by arterial spin labeling, brain glucose metabolism by <sup>18</sup>F-fluorodeoxyglucose (FDG) positron emission tomography, and activation of brain networks by functional MRI. Post- versus presurgery, we found a general increase of cerebral blood flow but a decrease of total brain FDG uptake during normoglycemia. During hypoglycemia, there was a marked increase in total brain FDG uptake, and this was similar for post- and presurgery, whereas hypothalamic FDG uptake was reduced during hypoglycemia. During hypoglycemia, attenuated responses of counterregulatory hormones and improvements in cognitive function were seen postsurgery. In early hypoglycemia, there was increased activation post- versus presurgery of neural networks in brain regions implicated in glucose regulation, such as the thalamus and hypothalamus.**

**The results suggest adaptive responses of the brain that contribute to lowering of glycemia following RYGB, and the underlying mechanisms should be further elucidated.**

The global rise in obesity and type 2 diabetes is one of the great challenges to public health in the 21st century. Results of bariatric surgery have shed light on several new and crucial mechanisms by which hunger, satiety, and body weight regulation, as well as glucose homeostasis, can be modified. Roux-en-Y gastric bypass (RYGB) is highly effective to prevent and reverse type 2 diabetes (1–3), with multiple pathways involved (e.g., hepatic glucose production, postprandial glucagon-like peptide 1 secretion, adipose factors) (4). Less is known about the role of neuroendocrine mechanisms and the central nervous system (CNS) in achieving favorable metabolic effects.

Besides these beneficial effects, RYGB surgery commonly leads to episodes of postprandial hypoglycemia (5), which are usually asymptomatic, pointing to an adaptive lowering of the glycemic “set point.” To some extent, this resembles the clinical phenomenon known as impaired awareness of hypoglycemia (IAH), which is observed in some patients with type 1 diabetes. These patients display

<sup>1</sup>Department of Medical Sciences, Clinical Diabetes and Metabolism, Uppsala University, Uppsala, Sweden

<sup>2</sup>Department of Surgical Sciences, Uppsala University, Uppsala, Sweden

<sup>3</sup>Department of Neurosciences and Department of Psychology, Uppsala University, Uppsala, Sweden

<sup>4</sup>Department of Radiation Sciences, Umeå University, Umeå, Sweden

<sup>5</sup>Faculty of Medicine, University of Geneva, Geneva, Switzerland

Corresponding author: Jan W. Eriksson, [jan.eriksson@medsci.uu.se](mailto:jan.eriksson@medsci.uu.se)

Received 19 November 2020 and accepted 25 February 2021

This article contains supplementary material online at <https://doi.org/10.2337/figshare.14114159>.

K.E.A. and M.H.L. contributed equally.

© 2021 by the American Diabetes Association. Readers may use this article as long as the work is properly cited, the use is educational and not for profit, and the work is not altered. More information is available at <https://www.diabetesjournals.org/content/license>

**See accompanying article, p. 1244.**

attenuation of symptoms and some counterregulatory hormonal responses during hypoglycemia compared with patients with normal hypoglycemic awareness (6). Moreover, a blunting of responses to hypoglycemia have been found in IAH in brain regions involved in hypoglycemic counterregulation, including the thalamus, hypothalamus, and brain stem and regions involved in behavioral responses, such as the striatum, amygdala, and various cortical regions (7–10).

Interestingly, attenuation of hormonal and symptomatic responses to hypoglycemia has also been observed after RYGB (11,12). In obesity and type 2 diabetes, positron emission tomography (PET) investigations performed during euglycemic-hyperinsulinemic clamp showed elevated brain glucose uptake (13,14), and this can be normalized after RYGB (15). While IAH can impair both short- and long-term cognitive performance (16,17), less is known about cognition in relation to hypoglycemia after bariatric surgery (12). In the current study, we combined hormonal, cognitive, and neuroimaging assessments during normoglycemic and hypoglycemic clamps in subjects before and after RYGB surgery.

**RESEARCH DESIGN AND METHODS**

This study was conducted at Uppsala University and Uppsala University Hospital. Subjects aged 18–60 years with a BMI of 35–45 kg/m<sup>2</sup> were recruited after a regular visit at the obesity outpatient clinic before planned bariatric surgery. Main exclusion criteria were diagnosis of diabetes, history of cardiovascular events, contraindication to PET/MRI investigation, treatment with β-blockers or CNS-active drugs, and serious psychiatric or substance abuse disorders.

The subjects came for two study visits: before RYGB (median 41 days, range 20–76 days) and then ~4 months (median 130 days, range 106–155 days) after RYGB. In accordance with local clinical guidelines, subjects received a 4-week low-caloric diet of 800–1,100 kcal/day before the RYGB, which was performed laparoscopically at the Department of Surgery, Uppsala University Hospital. On both study visits, subjects came to the PET/MR facility at 8:00 A.M. after an overnight fast. Medical history, anthropometric measures, and blood samples were obtained. Total body fat was assessed with bioimpedance (Body Composition Analyzer BC-418; Tanita).

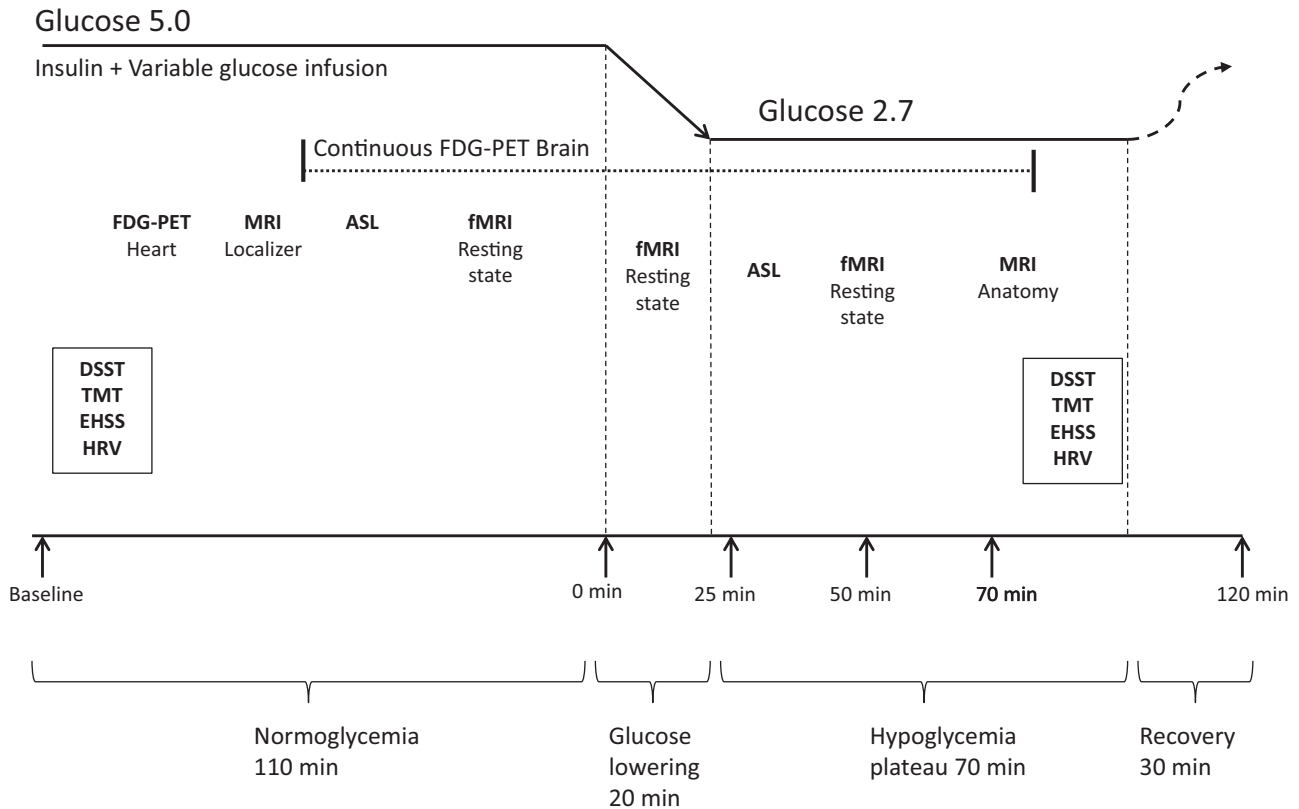


**Figure 1**—Schematic overview of the clamp and imaging investigations performed pre- and post-RYGB. Arrows at the bottom indicate time points for hormone blood samples. ASL, arterial spin labeling; DSST, Digital Symbol Substitution Test; EHSS, Edinburg Hypoglycemia Symptom Scale; HRV, heart rate variability; TMT, Trail Making Test.

### Glucose Clamp Procedure

A schematic overview is given in Fig. 1. After blood sampling and physical examinations, the hyperinsulinemic glucose clamp started with simultaneous infusion of insulin and 20% glucose. Potassium was infused with a target rate of 8 mmol/h in order to avoid insulin-induced hypokalemia. After priming, insulin (Actrapid; Novo Nordisk, Copenhagen, Denmark) was infused at a steady-state rate of 80 mU/m<sup>2</sup> body surface area/min, and the rate of 20% glucose infusion was adjusted on the basis of plasma glucose readings every 5 min. During the normoglycemic phase, the target glucose level was 5.0 mmol/L, and assessments of heart rate variability (HRV), cognitive function, and hypoglycemic symptoms (Edinburgh Hypoglycemia Symptom Score [EHSS]) were performed. Approximately 30 min into the clamp, the subject was positioned in the PET/MR scanner. After an additional 30 min, <sup>18</sup>F-fluorodeoxyglucose (FDG) was rapidly infused, and PET scanning was initiated followed by arterial spin labeling (ASL) and functional MRI (fMRI), as depicted in Fig. 1. After another 50 min, plasma glucose was lowered by temporarily stopping the glucose infusion. The target was 2.7 mmol/L, which was typically reached at ~20 min, and this was then maintained for 70 min. FDG-PET, ASL, and fMRI were performed again. After ~50 min, subjects exited the scanner, and HRV, cognitive function, and EHSS assessments were again performed. The recovery phase was initiated by stopping the insulin infusion while the glucose infusion continued for 30 min at a fixed rate of 100 mg/kg body weight/h. Because of the complex technical procedures, sometimes there were slight delays in experimental periods (Table 1) and sampling times.

### Cardiovascular Function

To assess autonomic nervous system activity, HRV was assessed for 6 min during normoglycemia and during late hypoglycemia in the supine position, using a single-channel electrocardiogram system (Actiwave Cardio; CamNtech Ltd., Fenstanton, U.K.), and a power spectrum analysis of HRV was performed (18). Blood pressure was measured at rest before clamps. Heart rate was measured during the normoglycemic and hypoglycemic clamps.

### Cognitive Tests and Hypoglycemic Symptoms Scores

The Trail Making Test (TMT) (19) and Digit Symbol Substitution Test (DSST) (20) were performed during both the normoglycemic and the hypoglycemic phase of the clamp (19,20). To avoid bias as a result of learning effects, both the TMT and the DSST were sent by mail to the subjects before each investigation day with instructions to practice taking the tests. The TMT examines visual search, scanning, speed of processing, mental flexibility, and executive functions (21), while the DSST aims to measure cognitive operations, such as motor speed, attention, visuo-perceptual functions, and associative learning

(20). Hypoglycemic symptoms were assessed with the EHSS questionnaire (22) both in the normo- and hypoglycemic clamp phases.

### Biochemical Measurements

Blood samples were repeatedly drawn from an antecubital vein (Fig. 1) following arterialization using a heating pad. Analyses were performed at the Department of Clinical Chemistry and the Clinical Diabetes Research Laboratory of Uppsala University Hospital. Glucose during clamps was assessed with a Contour hand-held glucometer (Bayer). Insulin, C-peptide, and cortisol were determined with a cobas e analyzer (Roche), growth hormone (GH) and ACTH with IMMULITE 2000 XPi (Siemens Healthineers), and glucagon with ELISA (#10-1271-01; Mercodia, Uppsala, Sweden).

### Brain Imaging Using PET, ASL, and fMRI

All examinations were performed using integrated PET/MR (SIGNA; GE Healthcare, Waukesha, WI), which combines a 3T MRI with a time-of-flight-capable silicone photomultiplier-based PET scanner (23). All subjects were scanned in supine position using an eight-channel head coil (MR Instruments, Inc., Minneapolis, MN). First, the subject was positioned with the field of view of the PET/MR centered over the heart. Simultaneously with a bolus injection of 2–3 MBq/kg FDG, a 10-min dynamic PET scan was started. Then, the subject was moved so that the brain was in the center of the field of view, and PET scanning was resumed at ~20 min postinjection and continued for ~120 min during normo- and hypoglycemia (Fig. 1). Arterialized venous blood samples were taken for measurement of radioactivity after the cardiac scan, prior to start of the brain scan, and repeatedly at set times during the remainder of the scan. PET image processing is described in the Supplementary Material.

A 3D fast-spin echo pseudo-continuous ASL with spiral readout and background suppression was acquired at a postlabel delay of 2,000 ms. In addition, the protocol included a high-resolution 3D T1-weighted image and a 3D T2-weighted fluid attenuated inversion recovery as anatomical references and a two-point Dixon sequence in combination with a zero echo time sequence for attenuation correction of PET data. ASL-derived cerebral blood flow (CBF) images were calculated according to the model defined by Buxton et al. (24) and recommended by Alsop et al. (25), including a correction term for full proton density reference (26–29).

fMRI during resting state implemented a standard echo-planar imaging sequence with the following fundamental parameters: whole-brain coverage, voxel size 3.4 × 3.4 × 3.0 mm<sup>3</sup>, 45 slices, 200 repetitions, repetition time 3.0 s, and echo time 3.0 ms. Analysis was carried out using tensorial independent component (IC) analysis (TICA) (30) and region of interest (ROI)-to-ROI analysis. TICA was implemented as in MELODIC

**Table 1—Anthropometric and biochemical measures at the presurgery visit and after gastric bypass (postsurgery)**

	Presurgery (n = 11)	Postsurgery (n = 11)	P value
<b>Anthropometry</b>			
Sex (male/female), n	3/8	—	—
Age (years)	35 (± 8)	—	—
Time from surgery to postsurgery visit 2 (days)	—	130 (122; 148)	—
Weight (kg)	113.8 (109.7; 132.5)	83.3 (77.2; 98.5)	<b>0.003</b>
BMI (kg/m <sup>2</sup> )	40.2 (± 3.6)	29.9 (± 4.0)	<b>&lt;0.001</b>
Waist (cm)	119 (± 10)	95 (± 10)	<b>&lt;0.001</b>
Waist/hip ratio	0.90 (0.86; 0.96)	0.88 (0.83; 0.90)	0.328
Total body fat (%)	44.4 (± 7.3)	34.0 (± 10.2)	<b>&lt;0.001</b>
SBP (mmHg)	125 (± 13)	118 (± 12)	0.138
DBP (mmHg)	80 (± 10)	73 (± 11)	0.076
Heart rate normo (bpm)*	74 (73; 78)	61 (59; 74)	<b>0.004</b>
Heart rate hypo (bpm)†	78 (70; 87)	65 (60; 80)	<b>0.021</b>
Duration of normoglycemic clamp (min)	118 (113; 129)	111 (109; 114)	0.373
Duration of hypoglycemic clamp (min)	85 (80; 93)	80 (79; 90)	0.765
<b>Test scores</b>			
EHSS normo	14.3 (2.3)	15.1 (3.9)	0.57
EHSS hypo	31.5 (8.4)	28.3 (7.5)	0.28
DSST normo	31.5 (13.4)	27.5 (7.1)	0.19
DSST hypo	24.3 (6.3)	27.5 (9.3)	<b>0.046</b>
TMT‡ normo	43.7 (11.9)	42.6 (14.3)	0.33
TMT‡ hypo	52.0 (19.7)	34.4 (10.5)	<b>0.009</b>
<b>Biochemistry</b>			
HbA <sub>1c</sub> (mmol/mol)	34 (34; 36)	33 (30; 34)	<b>0.011</b>
HbA <sub>1c</sub> (NGSP %)	5.3 (5.3; 5.4)	5.2 (4.9; 5.3)	<b>0.011</b>
P-glucose (mmol/L)	6.0 (± 0.5)	5.3 (± 0.5)	<b>&lt;0.001</b>
S-insulin (mU/L)	10.5 (5.7; 15.8)	7.2 (4.5; 13.8)	0.113
S-C-peptide (nmol/L)	1.20 (± 0.29)	0.79 (± 0.22)	<b>&lt;0.001</b>
HOMA-IR	2.7 (1.6; 4.3)	1.4 (1.0; 3.5)	<b>0.047</b>
P-HDL cholesterol (mmol/L)	0.99 (± 0.14)	0.97 (± 0.21)	0.651
P-LDL cholesterol (mmol/L)	3.11 (± 0.75)	2.15 (± 0.58)	<b>&lt;0.001</b>
P-triglycerides (mmol/L)	0.99 (0.92; 2.07)	0.79 (0.71; 1.14)	<b>0.016</b>
P-glucagon (pmol/L)	9.8 (5.9; 13.8)	6.2 (4.8; 9.4)	0.131
S-cortisol (nmol/L)	182 (165; 252)	214 (166; 271)	1.000
P-ACTH (nmol/L)	2.7 (2.3; 5.5)	1.8 (1.6; 2.2)	<b>0.005</b>
S-GH (μg/L)	0.16 (0.05; 1.18)	1.80 (0.10; 7.00)	<b>0.008</b>
M-value (mg/kg LBM/min)	7.55 (± 3.90)	8.63 (± 2.53)	0.352

Data are mean (± SD) if normally distributed or median (IQR) unless otherwise indicated. P values represent comparison with paired t tests (if normally distributed) or Wilcoxon signed rank tests between pre- and postsurgery. Boldface indicates significance at P < 0.05. bpm, beats/min; DBP, diastolic blood pressure; HOMA-IR, HOMA of insulin resistance; hypo, hypoglycemic phase of clamp; NGSP, National Glycohemoglobin Standardization Program; normo, normoglycemic phase of clamp; P, plasma; S, serum; SBP, systolic blood pressure. \*Incomplete data for four subjects. †Incomplete data for one subject. ‡TMT low value = better.

(Multivariate Exploratory Linear Decomposition into Independent Components) version 3.15, part of FSL (FMRIB Software Library, <https://www.fmrib.ox.ac.uk/fsl>), using standard parameters. All six runs (three presurgery, three postsurgery [see Fig. 1]) of each subject were included in one analysis. This data set of all runs in all subjects identified 20 ICs in a data-driven manner without a priori assumptions. Those 20 ICs were then default ordered by the amount of data variance explained by the ICs. The IC analysis provides a so-called S-mode (measure of activation of each component) in each run. For ROI-to-ROI analysis in the CONN toolbox (31) (<https://web.conn-toolbox.org>), standard parameters were used except for the additional definition of ROIs of the medial hypothalamus and lateral hypothalamus (LH) (32). The subject

S-modes of the 20 ICs were used as input data for the post hoc statistical analysis between groups using Graph-Pad Prism 5 software. Neuroimaging postprocessing details and software and the full set of acquisition parameters for MRI scans are provided in the Supplementary Material.

### Statistical Analysis

Data are presented as mean (± SD) or as median (interquartile range [IQR]) as indicated. For biochemical measurements, the area under the curve (AUC) and the ΔAUC from hypoglycemia 0–70 min was calculated using the trapezoid method. If sampling time was delayed because of practical reasons, the concentration at the intended time was interpolated from the adjacent measured values.

Differences in clinical and biochemical variables were analyzed using paired *t* tests or Wilcoxon signed rank tests as appropriate and specified. FDG-PET and ASL data were analyzed using paired *t* tests. Spearman correlations were performed between selected clinical and imaging measures.  $P < 0.05$  was considered statistically significant. Details regarding statistical software are provided in the Supplementary Material.

### Ethics

The study was approved by the Regional Research Ethics Committee of Uppsala (Dnr 2017/210). All subjects received written and verbal information prior to signing an informed consent form. The study was conducted in accordance with the Declaration of Helsinki.

### Data Availability

The data and study protocol are available upon request to the corresponding author.

## RESULTS

Eighteen subjects were recruited, seven of whom did not complete both visits for various reasons, including personal circumstances, difficulties gaining venous access, back pain, anxiety, or other discomfort during the imaging procedure and one patient's cancellation of surgery. Thus, 11 subjects (3 males and 8 females) completed both visits. Clinical characteristics pre- and postsurgery are summarized in Table 1. RYGB led to the expected metabolic improvements: weight loss of 30.3 kg, BMI reduction of 10.3 kg/m<sup>2</sup>, and significant lowering of fasting glucose and HbA<sub>1c</sub>.

### Cardiovascular Function

There was a significant decrease in heart rate after RYGB. This was found during both normo- and hypoglycemic clamp periods ( $P < 0.01$  and  $P < 0.05$ , respectively) (Table 1). There were no significant changes in blood pressure or HRV spectral components.

### Cognitive Tests and Hypoglycemic Symptoms

These results are shown in Table 1. The DSST and TMT results showed significant improvements during hypoglycemia for the postsurgery versus presurgery comparison ( $P < 0.05$  and  $P < 0.01$ , respectively). There were no differences during the normoglycemic phase. The EHSS symptom scores were similar postsurgery versus presurgery.

### Biochemical Measurements

Glucose and hormone levels are displayed in Table 1 and Fig. 2. Clamp glucose levels tended to be slightly lower post- versus presurgery ( $P = 0.137$  and  $P = 0.070$  for normo- and hypoglycemia, respectively). During the recovery phase, glucose levels rose less post- versus presurgery ( $P < 0.01$ ). Fasting C-peptide levels were lower

postsurgery but were suppressed similarly to presurgery during the clamp. Clamp insulin levels, mainly reflecting exogenous insulin, were slightly and significantly lower postsurgery. Glucagon, ACTH, cortisol, and GH all increased during the hypoglycemic clamp. Postsurgery, this increase was attenuated for glucagon ( $P < 0.01$ ) and numerically for ACTH and cortisol response ( $P = 0.08$  and  $P = 0.16$ , respectively, for  $\Delta$ AUC;  $P < 0.01$  and  $P = 0.08$ , respectively, for total AUC). Fasting ACTH in the morning was also lower after surgery ( $P < 0.01$ ). The GH response was augmented post- versus presurgery ( $P < 0.01$ ).

### FDG-PET

Results from the FDG-PET investigations are shown in Figs. 3 and 4. Both the global brain FDG net influx rate (Ki) and the estimated total uptake of glucose (MRglu) were somewhat lower post- versus presurgery during normoglycemia ( $P < 0.05$  for both) (Fig. 3A and B). Hypoglycemia led to an approximately fourfold increase in Ki ( $P < 0.001$ ) (Fig. 3A) both pre- and postsurgery. The magnitude of this increase did not differ significantly pre- versus postsurgery. The whole-brain PET images of a typical subject are depicted in Fig. 3C. This increase of Ki during hypoglycemia was evident in most parts of the brain both pre- and postsurgery (Figs. 3C and 4A and C). However, this was not seen in the hypothalamic area, where Ki instead decreased during hypoglycemia, and this response was less evident post- versus presurgery (Fig. 4B and D). In hypoglycemia, the lumped constant for FDG uptake in the brain is not defined, and, therefore, MRglu estimates are not reported.

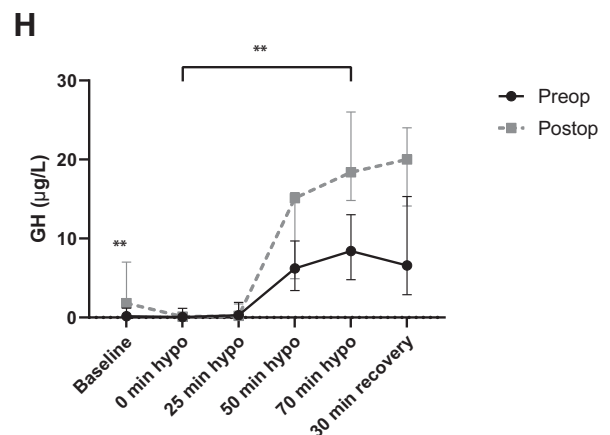
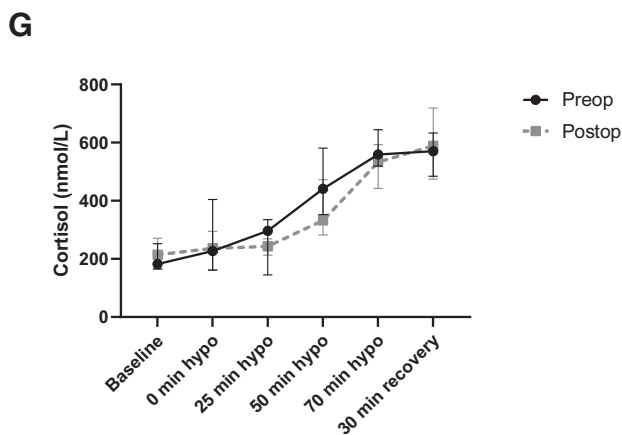
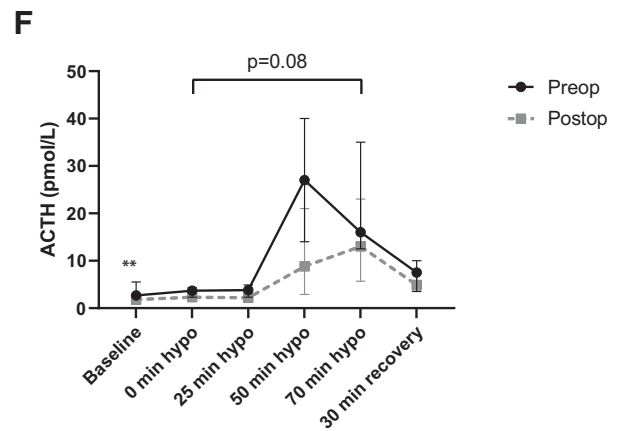
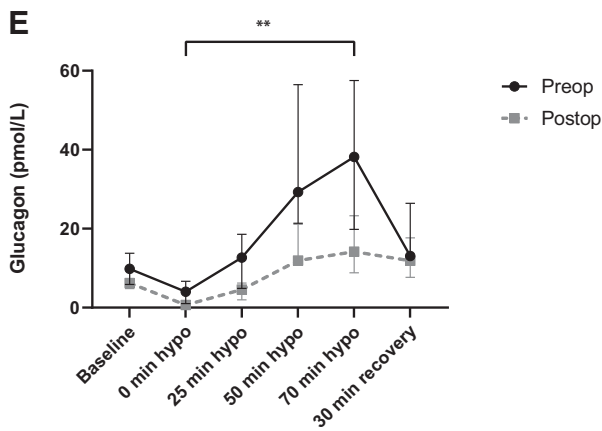
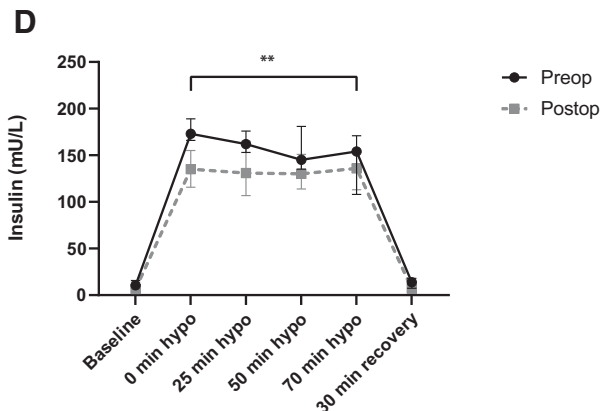
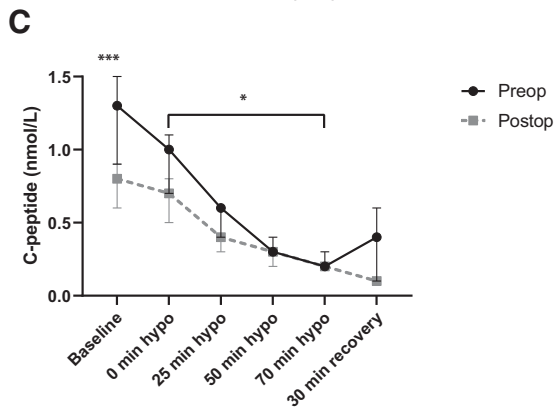
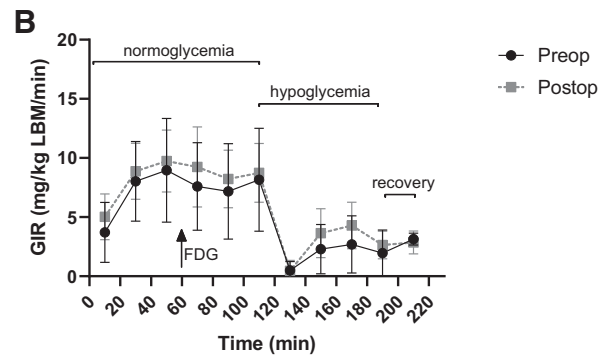
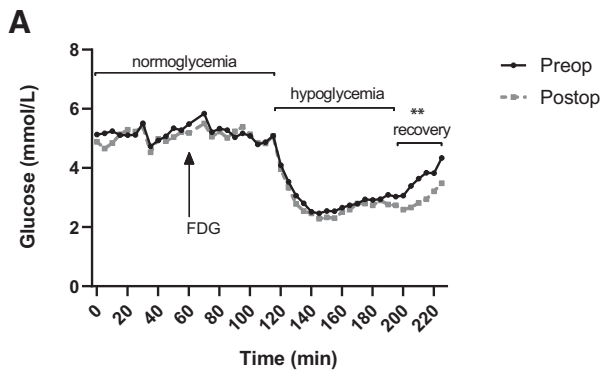
### CBF

Regional CBF was assessed with ASL, and data are summarized in Fig. 5. Postsurgery, CBF during the normoglycemic phase increased significantly in all brain regions. No significant changes were found between the normo- and hypoglycemic states pre- or postsurgery.

To assess whether the increased blood flow postsurgery was specific for the brain, we also used FDG-PET scanning of the heart to calculate whole-body arterial blood-flow, i.e., cardiac output (33). In absolute terms, cardiac output (in L/min) was clearly reduced after gastric bypass surgery, whereas the cardiac index (adjusted to body surface area) was not significantly altered (mean 3.06 vs. 3.23 L/m<sup>2</sup>/min for pre- vs. postsurgery, respectively).

### fMRI

Resting state fMRI was performed in three sequential periods during the clamp investigation: normoglycemia, early hypoglycemia and steady-state hypoglycemia (Fig. 1), and this was done before as well as after RYGB. TICA of MRI using the FSL software package (30) revealed one independent component (IC), which represents a functional connectivity resting-state network, explaining most variability of the data across all fMRI runs. This IC notably



includes bilateral thalamus and hypothalamus and, to a lesser degree, right dominant frontal regions (Fig. 6A). The activity of this IC (S-mode) was significantly higher post- versus presurgery during those runs in which blood glucose was rapidly lowered, i.e., during the early hypoglycemic clamp phase ( $P < 0.05$ ) (Fig. 6A and B).

The additional connectivity analysis was based on ROI-to-ROI analysis in the CONN toolbox using the right lateral hypothalamus (LH) (31) as the seed region. During early hypoglycemia, we observed a significantly decreased functional connectivity to left hippocampus and significantly increased functional connectivity to the cerebellar vermis regions 4 and 5 for the post- versus presurgery condition (Fig. 6C).

### Correlation Analyses

There were significant correlations between EHSS score and whole-brain CBF during hypoglycemia, particularly at the postsurgery investigation ( $\rho = 0.706$ ,  $P = 0.015$ ). Likewise, there were positive associations between cognitive function and CBF during hypoglycemia, both pre- and post-RYGB ( $P = 0.010$  and  $P = 0.079$ , respectively, for TMT;  $P = 0.017$  and  $P = 0.040$ , respectively, for DSST). These latter associations were seen for CBF in several separate regions but were significant only for the basal ganglia and hippocampus (data not shown). Whole-brain FDG uptake did not correlate with any of these scores. There were no significant correlations between postsurgery changes in anthropometric measures and changes in EHSS and cognitive scores or hormonal and fMRI responses to hypoglycemia. Furthermore, time since surgery did not correlate with changes in any of the above measures.

## DISCUSSION

This study demonstrates the feasibility of simultaneous metabolic and multimodal neuroimaging assessments. The findings indicate that changes in the brain's neuronal network activity, cognitive functions, as well as blood flow and energy metabolism occur after RYGB surgery in patients with severe obesity. Some RYGB effects were also found during experimental hypoglycemia, mainly on cognitive, hormonal, and fMRI readouts, and they may be of relevance for the asymptomatic hypoglycemic episodes that frequently occur in patients after RYGB (5). A nearly global attenuation of neurohormonal responses to hypoglycemia was found after RYGB, and this is likely largely due to adaptive changes within the brain. Conversely, such an adaptation is also likely to contribute to an overall lowering of glycemia and, hence, to the prevention, or

reversal, of type 2 diabetes in patients undergoing RYGB. The mechanisms behind this adaptation to low glucose levels remain elusive but may include upregulation of glucose transport into some brain regions, utilization of alternative fuels, and alterations of hypothalamic signaling and opioid-dependent pathways (34).

### Cognitive Function

Both cognitive tests, TMT and DSST, showed congruent results, with scores during hypoglycemia improving post-compared with presurgery. This is compatible with an adaptation of the brain to low glucose, leading to less vulnerability of cognition during hypoglycemia. Previous studies have also reported modulation of other aspects of cognitive function following RYGB, including problem solving and pattern comparison (12,35).

### Hormonal and Cardiovascular Responses

RYGB led to attenuated responses of counterregulatory hormones as well as heart rate during hypoglycemia. The blunted hormonal responses included glucagon, ACTH, and cortisol but, as reported previously (11,12), GH had a greater response following weight loss. After RYGB, glucose levels rose more slowly during the recovery phase directly after the hypoglycemic clamp, and this is most likely a consequence of the attenuated counterregulation. The finding following RYGB of a suppressed ACTH response to hypoglycemia provides additional support for a brain-mediated neuroendocrine adaptation, including the hypothalamic-pituitary-adrenal axis. Interestingly, in a recent study, we reported that enhanced counterregulatory responses are a feature of subjects with obesity and insulin resistance that might promote relative hyperglycemia and development of type 2 diabetes (36). In contrast, RYGB instead leads to an attenuated counterregulation, probably even below normal, which can contribute to the prevention or reversal of diabetes (11,12).

In our limited cohort, we did not see a significant improvement of whole-body insulin resistance, pointing to other mechanisms for the rapid glycemic effects of RYGB, such as reduced endogenous glucose production (37). Local insulin resistance in the brain has been implicated in obesity and type 2 diabetes (38). Some of the effects on brain functions and counterregulation found after RYGB in our study may be linked to improved brain insulin resistance, but this was not directly addressed and warrants further work.

In this study, we did not see any clear post-RYGB effect on autonomic nervous system reactivity during hypoglycemia, which is different from our previous report, indicating a blunted response of the sympathetic

**Figure 2—A–H:** Glucose levels, glucose infusion rates, and hormone levels during normoglycemic and hypoglycemic clamp. Data are median  $\pm$  IQR (all but panel A) or mean  $\pm$  SD (A). \* $P < 0.05$ , \*\* $P < 0.01$ , \*\*\* $P < 0.001$ .  $P$  values refer to differences between pre- and postsurgery, during the hypoglycemic period (brackets, AUCs) or fasting levels (baseline).  $P$  values within brackets refer to Wilcoxon signed rank tests of  $\Delta$ AUC (for all panels except D, where total AUC is shown). GIR, glucose infusion rate; hypo, hypoglycemic phase of clamp; LBM, lean body mass; Preop, preoperative; Postop, postoperative.

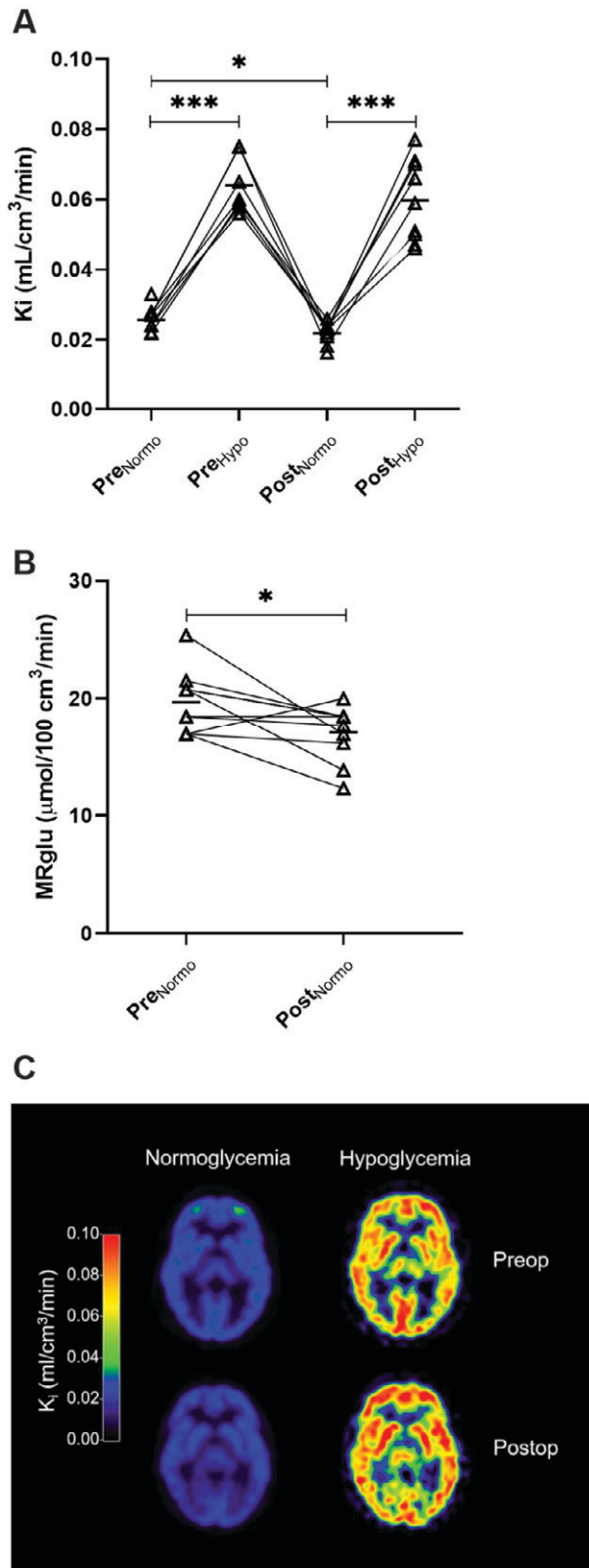


**Figure 3**—FDG PET of the brain. **A**: Whole-brain  $K_i$  values during normo- and hypoglycemia. **B**: MRglu during normoglycemia. **C**: Ki PET images for a typical patient pre- and postsurgery during normo- and hypoglycemia. Data in panels **A** and **B** presented as spaghetti plot of individual values with individual connecting lines and mean of all subjects at that time point (horizontal solid lines).  $n = 11$ .

nervous system (11). This is probably explained by HRV assessments now being done only in the very last part of the hypoglycemic period as opposed to continuous registration.

### CBF, fMRI, and FDG-PET

The counterregulatory response to hypoglycemia is largely coordinated by the basal regions of the brain, in particular the hypothalamus (34). It is therefore intriguing that we found an increased activity on resting-state fMRI assessments in these regions as well as some others during hypoglycemia post- versus presurgery. Although the functional consequences of increased neural activity in these brain regions are unclear, it may be hypothesized that this network exerts an inhibitory effect on hypoglycemic counterregulation. A causal connection between such findings and the attenuated neurohormonal counterregulation reported in this and a few previous studies (11,12) is therefore plausible and intuitively appealing. However, it is beyond the reach of our current results to allow firm conclusions about this connection.

A major finding of the ASL investigations was a general increase in blood flow in all brain regions occurring after RYGB, and this was largely seen during both normoglycemia and hypoglycemia. Interestingly, we found a link between increased brain blood flow during hypoglycemia and better results on cognitive tests, compatible with a potential impact of blood flow vis-à-vis cognitive improvement following RYGB. Since there was no significant post-surgery effect on whole-body blood flow (cardiac index), we propose that the increase in CBF is secondary to effects on regional vasoregulation. Of note, impaired vasoreactivity has been reported in obese versus lean subjects, but it was rapidly normalized after RYGB (39).

In contrast to blood flow, glucose metabolic rate, as reflected by FDG uptake, in the brain dropped after RYGB when measured during normoglycemia. This is compatible with previous findings by other investigators (13,15,37) showing elevated brain glucose uptake in obese subjects during hyperinsulinemic-normoglycemic clamps and a normalization following bariatric surgery. As expected, we found an increased plasma clearance of FDG by the brain ( $K_i$ ), and thus extraction fraction, during hypo- versus normoglycemia. However,  $K_i$  during hypoglycemia did not change after RYGB, and the MRglu could not be calculated because the assigned lumped constant for FDG of 0.65 during normoglycemia (14,40) is probably not applicable for hypoglycemia. This was shown in rats, where the deoxyglucose lumped constant of the brain was more

\* $P < 0.05$ , \*\*\* $P < 0.001$  for post- vs. presurgery (paired  $t$  tests). PreNormo and PostNormo: missing data for one subject; PreHypo: missing data for four subjects; PostHypo: missing data for two subjects.

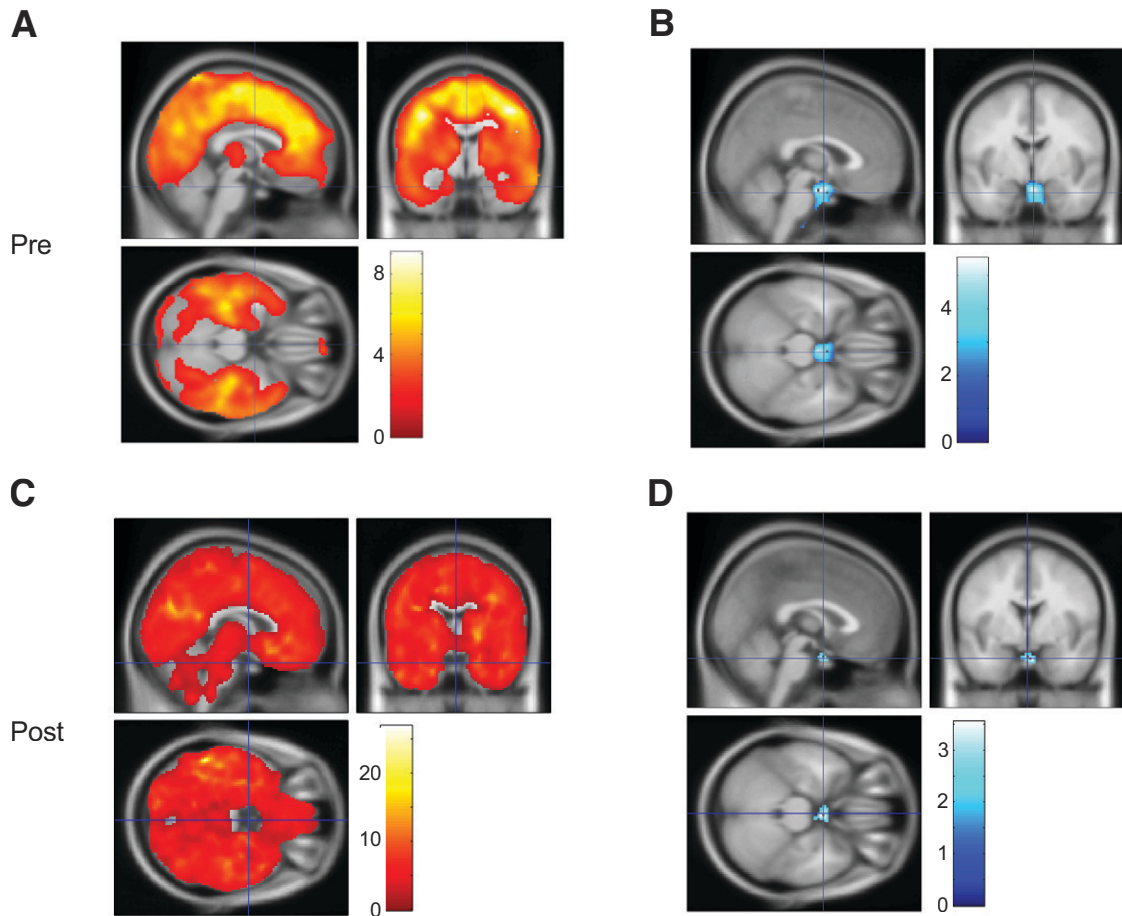


**Figure 4**—Difference in  $^{18}\text{F}$ -FDG net influx rates between hypo- and normoglycemic clamp periods. PET statistical parametric mapping (SPM) T-maps show comparisons from the presurgery (A and B) and postsurgery (C and D) investigations, respectively. A and C show clusters with significantly increased  $^{18}\text{F}$ -FDG net influx rate for hypo- vs. normoglycemia (red), whereas B and D show clusters with significant reduction (blue). The color maps represent T-values, indicating the number of pooled standard deviations between net influx rate values during hypo- vs. normoglycemia, where  $T > 1.96$  corresponds to  $P < 0.05$ . Minimum cluster size for significance was 50 voxels ( $0.4 \text{ cm}^3$ ). The crosshairs are centered on the hypothalamic cluster in panel B and the peak coordinates (MNI) are 0,  $-8$ ,  $-22$ .

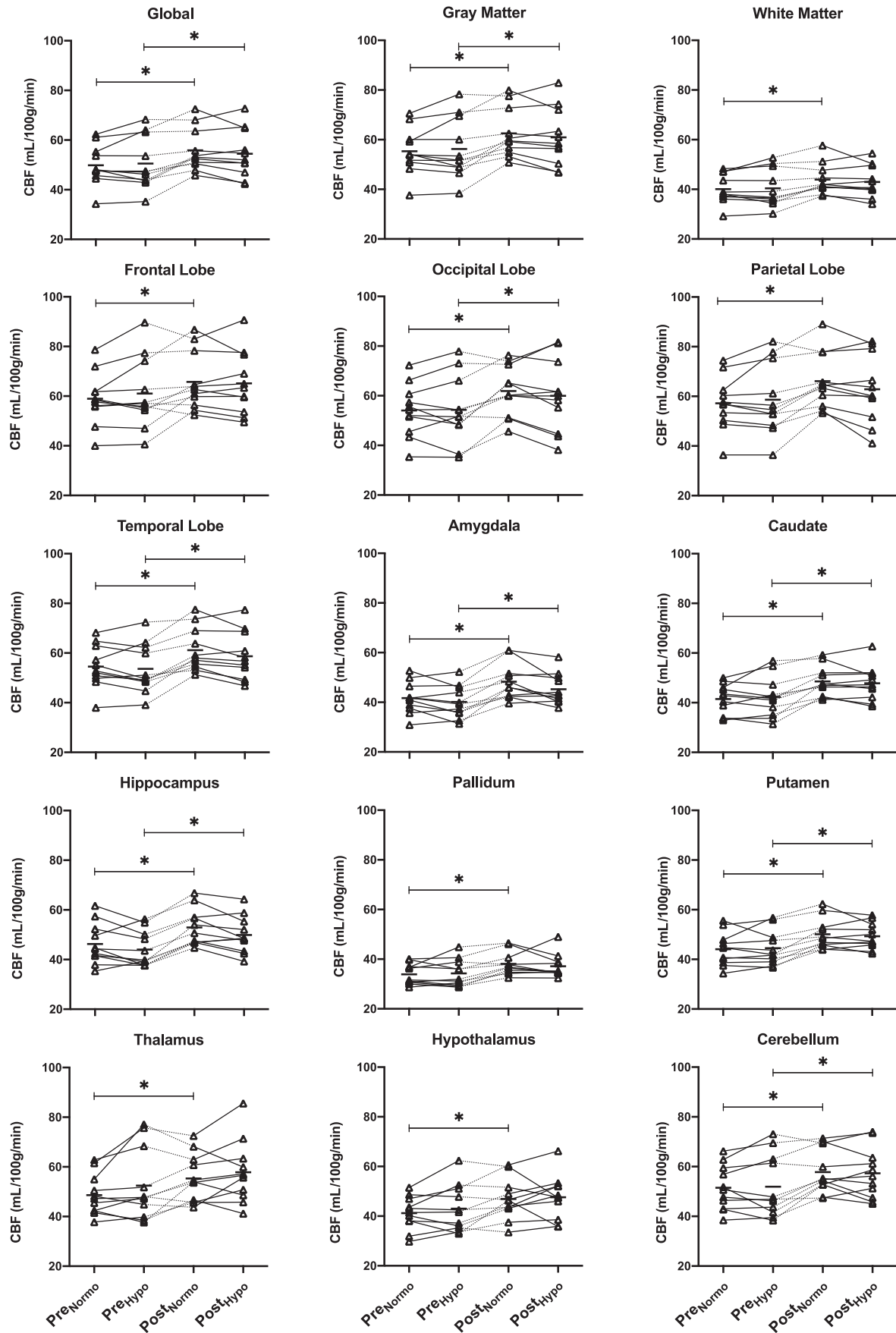
than twofold higher at plasma glucose 1.9 compared with 7 mmol/L (41). It might be assumed that the overall brain glucose uptake during modest hypoglycemia in our subjects was in a similar range as in normoglycemia and, most importantly, it did not change following RYGB.

In contrast to the whole brain, there was a decrease in the hypothalamic FDG uptake rate during hypoglycemia, and this decrease appeared to be less evident post- versus presurgery. These findings may point to an involvement of glucose uptake and, potentially, sensing in the hypothalamus coordination of counterregulatory neuroendocrine responses.

The somewhat lower  $K_i$  for FDG in normoglycemia post- versus presurgery may suggest an adaptation of the postsurgery brain to become less dependent on glucose uptake per se, possibly by metabolizing glucose more efficiently or utilizing alternative energy sources, including lactate and ketones. Indeed, intravenous administration of both lactate and  $\beta$ -hydroxybutyrate during

hypoglycemia has been shown to decrease symptoms, cognitive dysfunction, and hormonal counterregulation in healthy subjects (42).

Overall, further studies are needed to directly assess nutrient uptake and metabolism in the brain during hypoglycemia in normal subjects as well as in subjects with diabetes or obesity, also after bariatric surgery. In our present study, RYGB was followed by an altered neuronal network response to hypoglycemia in brain regions that are considered to be involved in the regulation of glucose turnover. This may contribute to the overall glucose-lowering effects of RYGB. A reduction of whole-brain glucose uptake was seen under normoglycemic conditions, and a rise in CBF was demonstrated in both normo- and hypoglycemia. Thus, it cannot be established whether the attenuation of counterregulation to hypoglycemia following RYGB is dependent on changes in brain glucose uptake and/or blood flow, and additional targeted and dynamic assessments of specific brain regions may be needed.



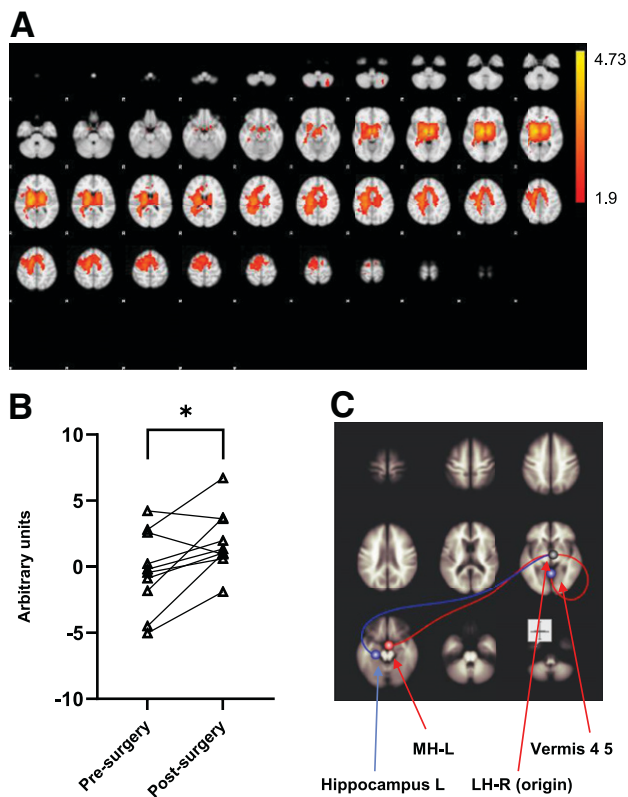


**Figure 6**—fMRI. **A:** TICA across all six resting fMRI runs revealed one IC, which represents a functional connectivity resting-state network, explaining most variability. This resting-state network was defined purely on the provided data without prior assumption and includes, notably, bilateral thalamus and hypothalamus. The activity of this IC was significantly higher after vs. before surgery (red color; S-mode) during the first 20 min of the hypoglycemic clamp (i.e., rapid glucose lowering) ( $P < 0.05$ ). The color code represents T-values. **B:** Individual data of the above IC activity (S-mode) during the initial phase of hypoglycemia.  $*P < 0.05$ . **C:** The ROI functional connectivity analysis using the right LH as seed region as defined on the basis of previous literature (31). During initial hypoglycemia, there was a significantly decreased functional connectivity to left hippocampus and a significantly increased functional connectivity to vermis regions 4 and 5 for the post- vs. presurgery condition. Similar increases in connectivity to corresponding regions were obtained using the left LH as seed region (data not shown).  $n = 10$ . L, left; LH, lateral hypothalamus; MH, medial hypothalamus; R, right.

### Limitations

This study protocol was laborious and challenging for patients as well as staff, and there was an  $\sim 30\%$  dropout rate among the included subjects. Therefore, the number of subjects completing the protocol was small ( $n = 11$ ). There were also some technical issues that led to fewer subjects for some assessments. The spatial resolution of our MR and PET exams did not allow for very detailed regional analysis, for example, at the subnucleus level of the

hypothalamus. Individual subnuclei can exert different and sometimes opposing effects on whole-body glucose turnover and energy balance (43), making the functional consequences of changes detected in hypothalamic glucose uptake or network activity uncertain. Furthermore, we have no results at present on anatomical assessments, and there may be structural effects in specific brain regions in addition to the functional changes. Previous work has suggested an increase in gray as well as white matter density in specific brain areas after RYGB, which may be related to the brain's regulation of energy balance (15,44,45). Importantly, there is yet limited understanding of the functional impact of changes in the brain's glucose uptake and blood flow rates that were found in our study.

### Conclusions

The current results suggest adaptation of the brain to lower glycemic levels following RYGB. This is supported by the attenuation of several insulin-antagonistic responses to hypoglycemia. In the brain, there were changes after RYGB in neural activation by hypoglycemia in central regions and the hypothalamus that are considered important for the coordination of glucose regulation. There were also global changes in brain glucose uptake rate and blood flow, and the latter may be related to improved cognitive function. Taken together, our findings point toward a role of the brain to orchestrate maintenance of normoglycemia and thereby reverse, or prevent, type 2 diabetes following gastric bypass surgery. Although critical hormonal and metabolic effects are finally exerted in the peripheral “end organs,” the glycemic set point may largely be determined and governed by the CNS.

**Acknowledgments.** The authors thank all study participants for their invaluable support. The authors are very grateful to research nurses Anna Åhlander, Sofia Löfving, Caroline Woxberg, and Carola Almström (all Department of Medical Sciences, Uppsala University) and Anders Lundberg, Marie Åhlman, and Gunilla Arvidsson (all Department of Surgical Sciences, Uppsala University). The authors also thank Prof. Elna-Marie Larsson (Department of Surgical Sciences, Uppsala University) for expert advice and support in the early phase of this study.

**Funding.** The study was funded by grants from the Swedish Diabetes Foundation (DIA2019-490), EXODIAB—Excellence of Diabetes Research in Sweden, the Ernfors Foundation, TREATMENT (EC H2020-MSCA-ITN-721236), Novo Nordisk Fonden (NNF200C0063864), and ALF—Swedish Government Research Grants to Uppsala University Hospital.

**Duality of Interest.** No potential conflicts of interest relevant to this article were reported.

**Author Contributions.** K.E.A. contributed to the study design, supervised the experiments, performed statistical analyses on clinical characteristics, collated results from co-authors, and wrote the manuscript. M.H.L. supervised experiments, performed statistical analyses on clinical

**Figure 5**—Regional CBF (by ASL) for normo- and hypoglycemia states in subjects pre- and postsurgery. Data are presented as spaghetti plots of individual values with individual connecting lines and mean of all subjects at that time point (horizontal solid lines).  $*P < 0.05$  (paired  $t$  tests,  $n = 11$ ). hypo, hypoglycemic phase of clamp; normo, normoglycemic phase of clamp; Pre, preoperative; Post, postoperative.

characteristics and cardiovascular function, collated results from co-authors, and wrote the manuscript. N.A. contributed to the study design and performed data preparation, statistical analyses, presentation, and interpretation of cognitive tests and symptoms. S.K. examined FDG-PET imaging, performed statistical analyses, and presented and interpreted the FDG-PET results. M.F. examined ASL images, performed statistical analyses, and presented and interpreted the ASL results. M.J.P. gave statistical advice, performed the statistical analyses on metabolism and hormones, and presented these results. M.G. contributed to the study design and aided in interpreting the cognitive tests and fMRI findings. F.A.K. contributed to the study design and interpretation of major findings. G.F. performed and interpreted statistical analyses. M.S. contributed to the study design and the interpretation of major findings. U.W. performed and interpreted the HRV analyses. S.H. examined the fMRI imaging, performed the statistical analyses, and interpreted and presented the results. M.L. contributed to the study design, examined the FDG-PET imaging, and interpreted and presented the results. J.W. contributed to the study design, examined the fMRI and ASL imaging, and interpreted the results. J.W.E. was the principal investigator and, as such, designed and coordinated the study, interpreted the findings, and wrote the manuscript. All authors critically revised and approved the final manuscript. J.W.E. is the guarantor of this work and, as such, had full access to the all the data in the study and takes responsibility for the integrity of the data and the accuracy of the data analysis.

## References

- Buchwald H, Estok R, Fahrenbach K, et al. Weight and type 2 diabetes after bariatric surgery: systematic review and meta-analysis. *Am J Med* 2009;122:248–256.e5
- Katsogiannis P, Kamble PG, Wiklund U, et al. Rapid changes in neuroendocrine regulation may contribute to reversal of type 2 diabetes after gastric bypass surgery. *Endocrine* 2020;67:344–353
- Sjöström L, Lindroos A-K, Peltonen M, et al.; Swedish Obese Subjects Study Scientific Group. Lifestyle, diabetes, and cardiovascular risk factors 10 years after bariatric surgery. *N Engl J Med* 2004;351:2683–2693
- Morínigo R, Moizé V, Musri M, et al. Glucagon-like peptide-1, peptide YY, hunger, and satiety after gastric bypass surgery in morbidly obese subjects. *J Clin Endocrinol Metab* 2006;91:1735–1740
- Abrahamsson N, Edén Engström B, Sundbom M, Karlsson FA. Hypoglycemia in everyday life after gastric bypass and duodenal switch. *Eur J Endocrinol* 2015;173:91–100
- Cryer PE. Hypoglycemia-associated autonomic failure in diabetes. *Am J Physiol Endocrinol Metab* 2001;281:E1115–E1121
- Mangia S, Tesfaye N, De Martino F, et al. Hypoglycemia-induced increases in thalamic cerebral blood flow are blunted in subjects with type 1 diabetes and hypoglycemia unawareness. *J Cereb Blood Flow Metab* 2012;32:2084–2090
- Dunn JT, Cranston I, Marsden PK, Amiel SA, Reed LJ. Attenuation of amygdala and frontal cortical responses to low blood glucose concentration in asymptomatic hypoglycemia in type 1 diabetes: a new player in hypoglycemia unawareness? *Diabetes* 2007;56:2766–2773
- Cranston I, Reed LJ, Marsden PK, Amiel SA. Changes in regional brain (18)F-fluorodeoxyglucose uptake at hypoglycemia in type 1 diabetic men associated with hypoglycemia unawareness and counter-regulatory failure. *Diabetes* 2001;50:2329–2336
- Hwang JJ, Parikh L, Lacadie C, et al. Hypoglycemia unawareness in type 1 diabetes suppresses brain responses to hypoglycemia. *J Clin Invest* 2018;128:1485–1495
- Abrahamsson N, Börjesson JL, Sundbom M, Wiklund U, Karlsson FA, Eriksson JW. Gastric bypass reduces symptoms and hormonal responses in hypoglycemia. *Diabetes* 2016;65:2667–2675
- Guldstrand M, Ahrén B, Wredling R, Backman L, Lins PE, Adamson U. Alteration of the counterregulatory responses to insulin-induced hypoglycemia and of cognitive function after massive weight reduction in severely obese subjects. *Metabolism* 2003;52:900–907
- Hirvonen J, Virtanen KA, Nummenmaa L, et al. Effects of insulin on brain glucose metabolism in impaired glucose tolerance. *Diabetes* 2011;60:443–447
- Boersma GJ, Johansson E, Pereira MJ, et al. Altered glucose uptake in muscle, visceral adipose tissue, and brain predict whole-body insulin resistance and may contribute to the development of type 2 diabetes: a combined PET/MR study. *Horm Metab Res* 2018;50:e10
- Tuulari JJ, Karlsson HK, Hirvonen J, et al. Weight loss after bariatric surgery reverses insulin-induced increases in brain glucose metabolism of the morbidly obese. *Diabetes* 2013;62:2747–2751
- Chaytor NS, Barbosa-Leiker C, Ryan CM, Germine LT, Hirsch IB, Weinstock RS. Clinically significant cognitive impairment in older adults with type 1 diabetes. *J Diabetes Complications* 2019;33:91–97
- Howorka K, Heger G, Schabmann A, Anderer P, Tribl G, Zeithofer J. Severe hypoglycaemia unawareness is associated with an early decrease in vigilance during hypoglycaemia. *Psychoneuroendocrinology* 1996;21:295–312
- Almby KE, Abrahamsson N, Lundqvist MH, et al. Effects of GLP-1 on counter-regulatory responses during hypoglycemia after GBP surgery. *Eur J Endocrinol* 2019;181:161–171
- Bowie CR, Harvey PD. Administration and interpretation of the Trail Making Test. *Nat Protoc* 2006;1:2277–2281
- Jaeger J. Digit symbol substitution test: the case for sensitivity over specificity in neuropsychological testing. *J Clin Psychopharmacol* 2018;38:513–519
- Tombaugh TN. Trail Making Test A and B: normative data stratified by age and education. *Arch Clin Neuropsychol* 2004;19:203–214
- Deary IJ, Hepburn DA, MacLeod KM, Frier BM. Partitioning the symptoms of hypoglycaemia using multi-sample confirmatory factor analysis. *Diabetologia* 1993;36:771–777
- Grant AM, Deller TW, Khalighi MM, Maramraju SH, Delso G, Levin CS. NEMA NU 2-2012 performance studies for the SiPM-based ToF-PET component of the GE SIGNA PET/MR system. *Med Phys* 2016;43:2334–2343
- Buxton RB, Frank LR, Wong EC, Siewert B, Warach S, Edelman RR. A general kinetic model for quantitative perfusion imaging with arterial spin labeling. *Magn Reson Med* 1998;40:383–396
- Alsop DC, Detre JA, Golay X, et al. Recommended implementation of arterial spin-labeled perfusion MRI for clinical applications: a consensus of the ISMRM perfusion study group and the European consortium for ASL in dementia. *Magn Reson Med* 2015;73:102–116
- Dai W, Robson PM, Shankaranarayanan A, Alsop DC. Reduced resolution transit delay prescan for quantitative continuous arterial spin labeling perfusion imaging. *Magn Reson Med* 2012;67:1252–1265
- Dai W, Shankaranarayanan A, Alsop DC. Volumetric measurement of perfusion and arterial transit delay using hadamard encoded continuous arterial spin labeling. *Magn Reson Med* 2013;69:1014–1022
- Maleki N, Dai W, Alsop DC. Optimization of background suppression for arterial spin labeling perfusion imaging. *MAGMA* 2012;25:127–133
- Dai W, Garcia D, de Bazelaire C, Alsop DC. Continuous flow-driven inversion for arterial spin labeling using pulsed radio frequency and gradient fields. *Magn Reson Med* 2008;60:1488–1497
- Beckmann CF, Smith SM. Tensorial extensions of independent component analysis for multisubject fMRI analysis. *Neuroimage* 2005;25:294–311
- Whitfield-Gabrieli S, Nieto-Castanon A. Conn: a functional connectivity toolbox for correlated and anticorrelated brain networks. *Brain Connect* 2012;2:125–141
- Li P, Shan H, Nie B, et al. Sleeve gastrectomy rescuing the altered functional connectivity of lateral but not medial hypothalamus in subjects with obesity. *Obes Surg* 2019;29:2191–2199

33. Sorensen J, Stahle E, Langstrom B, Frostfeldt G, Wikstrom G, Hedenstierna G: Simple and accurate assessment of forward cardiac output by use of 1-(11)C-acetate PET verified in a pig model. *J Nucl Med* 2003;44:1176–1183
34. Stanley S, Moheet A, Seaquist ER. Central mechanisms of glucose sensing and counterregulation in defense of hypoglycemia. *Endocr Rev* 2019;40:768–788
35. Saindane AM, Drane DL, Singh A, Wu J, Qiu D. Neuroimaging correlates of cognitive changes after bariatric surgery. *Surg Obes Relat Dis* 2020;16:119–127
36. Lundqvist MH, Almby K, Wiklund U, et al. Altered hormonal and autonomic nerve responses to hypo- and hyperglycaemia are found in overweight and insulin-resistant individuals and may contribute to the development of type 2 diabetes. *Diabetologia* 2021;64:641–655
37. Rebelos E, Immonen H, Bucci M, et al. Brain glucose uptake is associated with endogenous glucose production in obese patients before and after bariatric surgery and predicts metabolic outcome at follow-up. *Diabetes Obes Metab* 2019;21:218–226
38. Kullmann S, Valenta V, Wagner R, et al. Brain insulin sensitivity is linked to adiposity and body fat distribution. *Nat Commun* 2020;11:1841
39. Lind L, Zethelius B, Sundbom M, Edén Engström B, Karlsson FA. Vasoreactivity is rapidly improved in obese subjects after gastric bypass surgery. *Int J Obes* 2009;33:1390–1395
40. Wu HM, Bergsneider M, Glenn TC, et al. Measurement of the global lumped constant for 2-deoxy-2-[<sup>18</sup>F]fluoro-D-glucose in normal human brain using [<sup>15</sup>O]water and 2-deoxy-2-[<sup>18</sup>F]fluoro-D-glucose positron emission tomography imaging. A method with validation based on multiple methodologies. *Mol Imaging Biol* 2003;5:32–41
41. Suda S, Shinohara M, Miyaoka M, Lucignani G, Kennedy C, Sokoloff L. The lumped constant of the deoxyglucose method in hypoglycemia: effects of moderate hypoglycemia on local cerebral glucose utilization in the rat. *J Cereb Blood Flow Metab* 1990;10:499–509
42. Veneman T, Mitrakou A, Mokan M, Cryer P, Gerich J. Effect of hyperketonemia and hyperlacticacidemia on symptoms, cognitive dysfunction, and counterregulatory hormone responses during hypoglycemia in normal humans. *Diabetes* 1994;43:1311–1317
43. Lundqvist MH, Almby K, Abrahamsson N, Eriksson JW. Is the brain a key player in glucose regulation and development of type 2 diabetes? *Front Physiol* 2019;10:457
44. Rullmann M, Preusser S, Poppitz S, et al. Gastric-bypass surgery induced widespread neural plasticity of the obese human brain. *Neuroimage* 2018;172:853–863
45. Rullmann M, Preusser S, Poppitz S, et al. Adiposity related brain plasticity induced by bariatric surgery. *Front Hum Neurosci* 2019;13:290